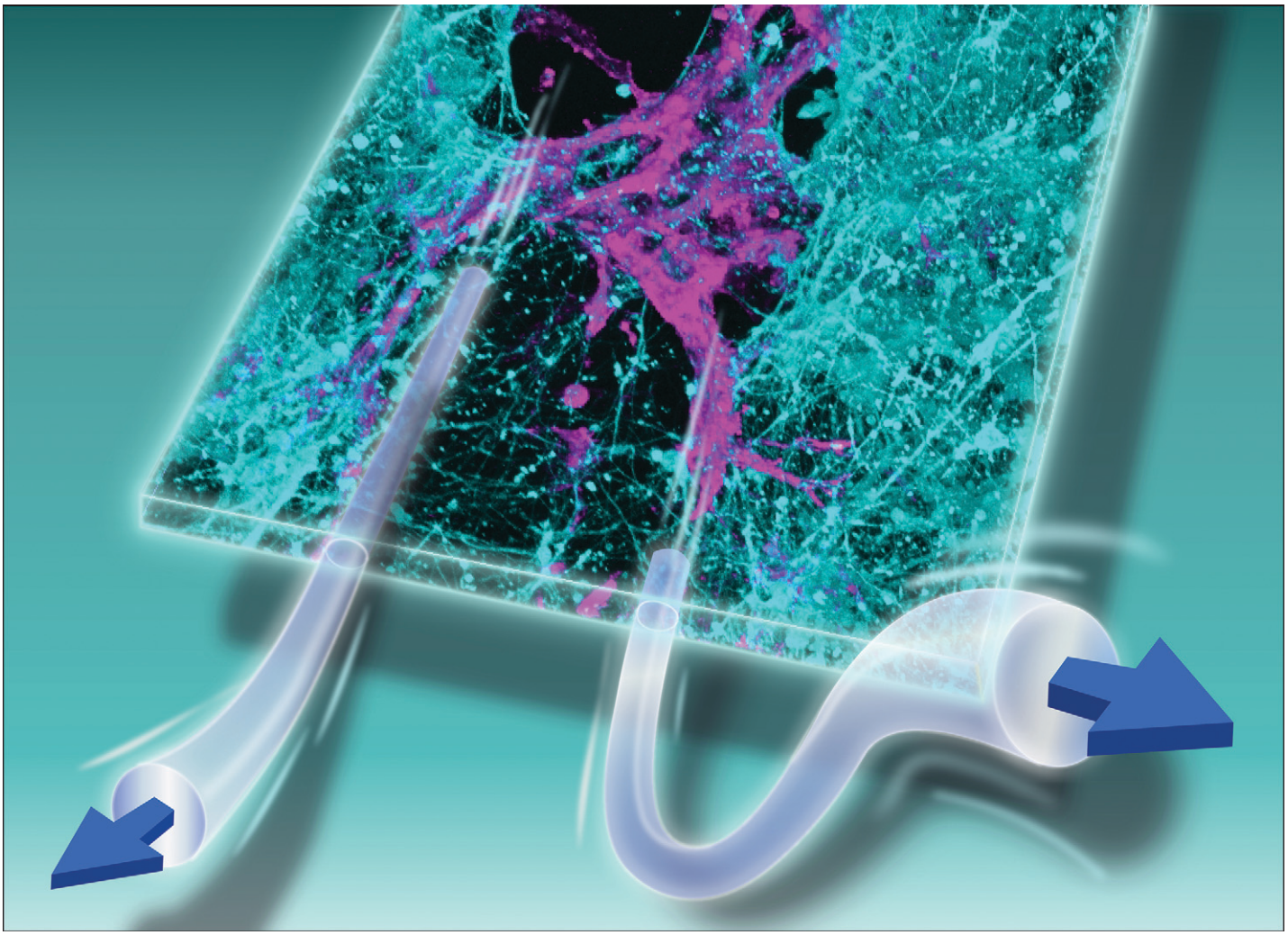

Featuring work from the team Macromolecules and Microsystems in Biology and Medicine (MMBM) of Institut Curie - UMR 168 and PSL Research University. The laboratory, located at Institut Pierre-Gilles de Gennes pour la Microfluidique in Paris, France, is focusing on the microfluidic developments for biomedical analysis and biophysical studies at cellular and tissular scales.

Transient microfluidic compartmentalization using actionable microfilaments for biochemical assays, cell culture and organs-on-chip

A simple compartmentalization approach was developed to transiently divide a microfluidic chamber into several compartments. This technology provides easy and low-cost solutions for constructing well-controlled microenvironments for biochemical and cellular assays.

As featured in:

See Ayako Yamada, Stéphanie Descroix *et al.*, *Lab Chip*, 2016, **16**, 4691.

ROYAL SOCIETY OF CHEMISTRY

www.rsc.org/loc

Registered charity number: 207890

Lab on a Chip

PAPER

View Article Online
View Journal | View Issue

Cite this: *Lab Chip*, 2016, **16**, 4691

Transient microfluidic compartmentalization using actionable microfilaments for biochemical assays, cell culture and organs-on-chip†

Ayako Yamada,*[abc] Renaud Renault,‡[abc] Aleksandra Chikina,‡[abc] Bastien Venzac,[abc] Iago Pereiro,[abc] Sylvie Coscoy,[ab] Marine Verhulsel,[abc] Maria Carla Parrini,[de] Catherine Villard,[abc] Jean-Louis Viovy[abc] and Stéphanie Descroix*[abc]

Received 13th September 2016,
Accepted 21st October 2016

DOI: 10.1039/c6lc01143h

www.rsc.org/loc

We report here a simple yet robust transient compartmentalization system for microfluidic platforms. Cylindrical microfilaments made of commercially available fishing lines are embedded in a microfluidic chamber and employed as removable walls, dividing the chamber into several compartments. These partitions allow tight sealing for hours, and can be removed at any time by longitudinal sliding with minimal hydrodynamic perturbation. This allows the easy implementation of various functions, previously impossible or requiring more complex instrumentation. In this study, we demonstrate the applications of our strategy, firstly to trigger chemical diffusion, then to make surface co-coating or cell co-culture on a two-dimensional substrate, and finally to form multiple cell-laden hydrogel compartments for three-dimensional cell co-culture in a microfluidic device. This technology provides easy and low-cost solutions, without the use of pneumatic valves or external equipment, for constructing well-controlled microenvironments for biochemical and cellular assays.

Introduction

Achieving a transient and controllable separation between different regions of a microfluidic chip is a functionality required in many applications that could involve molecules, cells or tissues. A widely used strategy for this purpose relies on the integration of pneumatic valves,[1] which are usually controlled by external pumps. This strategy offers high control over fluid manipulation but it tends to increase the complexity and fragility of the devices, while limiting their portability. In its original implementation, the valve-based technology only allows the sealing of narrow channels between chambers. Interesting generalizations were proposed,[2–4] but these approaches still require multilayer soft lithography and an external pressure control. SlipChip[5] or oil microsealing[6,7] can also be used for transient partitioning. However, these methods share the disadvantage of using oil, which is not favorable for some experiments, especially with living cells. Moreover, on a hydrophilic surface, oil partitioning does not provide a perfect sealing, whereas on a hydrophobic surface it leaves a layer of oil that can disturb further experiments.

Here, we propose an original and simple method, allowing the efficient transient partitioning of a microfluidic chamber into several compartments along centimeter lengths. Notably, this partition can be removed at any desired time in a quasi flow-free manner without external pumping systems. To achieve this compartmentalization, we use microfilaments of various sizes as removable partitions in conventional polydimethylsiloxane (PDMS) microfluidic chips. Depending on the desired applications, the bottom substrate can be a glass slide, a PDMS layer, or even a conventional culture dish to make it directly usable for biologists for on-chip cell culture. Microfilaments such as nylon fibers have been previously used in microfluidics as a mold to define cylindrical microchannels within PDMS or hydrogels,[8,9] while threads have been employed as matrices for capillarity-driven microfluidics.[10–12] However, they have never been used as a transient partition for a microfluidic device until our recent work, in which neuronal cell bodies were successfully separated from an axonal area using this strategy.[13] In this article, we further explore the implementation of this approach in diverse and more complex configurations, and demonstrate its potential for a wide range of applications. In particular, we

[a] *Laboratoire Physico Chimie Curie, Institut Curie, PSL Research University, CNRS UMR168, 75005, Paris, France. E-mail: ayako.yamada@curie.fr, stephanie.descroix@curie.fr*
[b] *Sorbonne Universités, UPMC Univ Paris 06, 75005, Paris, France*
[c] *Institut Pierre-Gilles de Gennes, 75005, Paris, France*
[d] *Institut Curie, Centre de Recherche, PSL Research University, 75005, Paris, France*
[e] *ART group, Inserm U830, 75248 Paris, France*

† Electronic supplementary information (ESI) available: Fig. S1–S6, Text S1, Movie S1. See DOI: 10.1039/c6lc01143h

‡ Equal contribution.

demonstrate the suitability of our method for (i) triggerable chemical diffusion, (ii) surface co-coating, (iii) two-dimensional (2D) cell co-culture, and (iv) hydrogel compartmentalization for 3D cell co-culture, showing its high versatility for biological, biochemical, and biophysical studies.

Microfluidics is a powerful approach to dynamically control fluidic environments in a channel, *e.g.* for dynamic chemical stimulations. Pumps or valves are widely used to exchange fluids in channels,[1,14,15] whereas the displacement of laminar flow boundaries has also been applied to rapidly switch the microenvironment at given locations in a channel.[16] In these approaches, it is necessary to keep fluids flowing. This is not suitable for all studies, notably for the study of cells or objects sensitive to shear stress, or for precious reagents. To overcome these problems, several shear-free devices have been developed. For instance, microchannels[17] or a nanoporous membrane[18] were employed to separate a main channel from flows containing the reagents to be dispensed by diffusion. Alternatively, micro-wells etched at the bottom of a channel were used to protect samples from flows.[19] However, these approaches still need an external fluidic control and elaborate fabrication processes. One of the interesting features of the compartmentalization strategy proposed here is the possibility to open at will a large fluidic communication to trigger chemical diffusion from one to the other transient compartment with minimal flow displacement. This is tested here by developing a free diffusion experiment, in which diffusion is triggered simply by removing the microfilament at any desired moment and without need of pumps.

The principle of our transient partitioning can be used also for molecular deposition on a 2D substrate at defined areas in a microfluidic chamber. Substrates specifically coated with biomolecules or synthetic molecules are widely used in cell biology or biophysics to elucidate cellular responses mediated by molecular recognitions, such as growth, adhesion, or migration.[20] Various strategies have thus been developed to define patterns of molecules, such as microcontact printing,[21] photolithography,[22,23] and UV-induced patterning.[24,25] Microfluidic approaches can also be used to pattern a substrate with differently coated areas by using laminar flows or by diffusion through microchannels.[26,27] This strategy is useful, for example, to compare the behaviors of large cell populations depending on the coating molecules in a single microfluidic channel. However, it requires fluid handling with a pressure control, and the coating density profile is continuously varying in space due to the combination of convection and diffusion. The spatial resolution is thus not as high as in the techniques described previously. In contrast, our transient partition strategy offers a versatile method for surface co-coating for cellular or biochemical assays in a microfluidic chamber, but does not share the limitations of flow-based patterning.

Our approach is also suited for seeding and culturing different cell populations on a 2D surface with a sharp interface in a single chamber. For applications such as cell co-cultures or invasion assays between two cell populations, silicone inserts from Ibidi, for example, have been widely used.[28–31] This method to seed cells in restricted regions relies on the same principle as used in stencils: the areas on which cells are unwanted are covered with a PDMS block[32] or microstencils made of PDMS or silicon.[33,34] This technique is convenient for cell cultures on an open substrate, but for closed microfluidic devices it requires an additional and delicate alignment of the channels with the cellular pattern. In contrast, our transient partition strategy allows the direct deposition of different cell types at different locations inside a microfluidic chamber without the need for alignment, while taking advantages of microfluidics, *i.e.* reduced consumption of cells and reagents, reduced system size including the gap between cell populations, and well-controlled microenvironment.

Besides 2D cell culture, which still remains a standard for various applications, growing evidence shows the importance of 3D cell culture in hydrogels mimicking extracellular matrices (ECM).[35,36] 3D culture is closer to the physiological situation for many cell types and "organs-on-chips" applications, and cell morphology or gene expression levels of certain proteins are generally altered between 2D and 3D culture configurations.[37] Microfluidics has been recognized as a promising technology for preparing hydrogel micro-compartments for 3D cell culture, and imposing geometrical configurations impossible to achieve with conventional culture methods. However, obtaining this compartmentalization still raises a number of challenges. One strategy consists in gelling fluids introduced by laminar flows, resulting in multi-component parallel hydrogels.[38,39] This approach, however, requires an accurate adjustment of the flow rates and viscosities of the flowing solutions, making it delicate to implement, and limiting applications. An alternative is the use of micro-pillars and tuned wetting properties to maintain hydrogels in predefined compartments, but the wettability of the chip substrate and the pressure applied to hydrogel solutions have to be carefully adjusted.[40,41] Although these devices are relatively easy to fabricate and use, the presence of pillars can affect the behavior of cells. It also limits the observation window and the size of free interfaces, and finally restricts the available configurations. There is thus a strong need to develop new methods to produce hydrogel micro-compartments of precise composition at predefined positions in microfluidic chips as a biomimetic 3D microenvironment. The strategy presented here offers an easy solution to fabricate parallel, adjacent, and centimeter-long hydrogel compartments containing different cell types. We show in particular a spatially-controlled 3D co-culture of mouse primary neurons and glial cells in ECM-like hydrogel, as well as the formation of collagen gel with a stepwise gradient.

In this article, we analyze the performance of this new transient compartmentalization approach compatible with various substrates, and demonstrate how the unique aspects of this technology enable new more favorable ways to tackle a broad range of microfluidics challenges, ranging from shear-free experiments to 3D cell co-culture.

Materials and methods

All reagents were purchased from Sigma-Aldrich unless otherwise specified.

Microfluidic chip preparation

An 80 μm-thick mold for an 80 μm-high microfluidic chamber was prepared as follows. A layer of SU-8 2050 (MicroChem) was formed on a 2 inch silicon wafer (Neyco) by spin-coating (TP6000, SET) at 2000 rpm for 30 s. After a soft bake, the wafer was exposed to UV light (MJB4 Mask Aligner) through a transparency mask prior to a post-exposure bake, and developed by SU-8 developer (MicroChem). To obtain a 300 μm-thick mold, 15, 100, and 200 μm-thick dry films (ADEX TDFS A15, EP SUEX TDFS D100 and D200, DJ DevCorp) were stuck on a 4 inch silicon wafer (Neyco) using laminator (DH-360, Linea) at the lamination speed 0.2 m min^{-1} and the temperature at 66 °C. After laminating each film, the wafer was heated at 85 °C for 2 min. The wafer was then exposed to UV light (UV-KUB 2, KLOÉ) through a transparency mask prior to a post-exposure bake, developed by SU-8 developer, and heated at 200 °C for 10 min. The photomasks were either purchased from Selba S. A. or printed by photoplotter (Filmstar Photoplotter, Bungard). The obtained molds were exposed to the vapor of trimethylchlorosilane (ABCR GmbH & Co. KG) for 5 min once, and used repeatedly without further treatment. The heights of the molds were measured to be 82.8 ± 3.0 μm and 303.3 ± 5.8 μm, respectively, by profilometer (Wyko NT1100, Veeco). PDMS and its curing agent (Sylgard 184 silicone elastomer kit, Dow Corning) were mixed at the ratio of 10 : 1 (w/w), poured on the mold, degassed, and reticulated at 80 °C for at least 2 h. A PDMS block, about 6 mm thick, was cut off from the mold and reservoirs and smaller inlets were punched in it using a 4 mm and 2 mm-diameter biopsy punches (Kai Industries), respectively. Fishing lines (MORRIS) made of fluorocarbon (VARIVAS Fluoro carbon Super tippet 9X 0.086 mm diameter, VARIVAS Super Tippet Master Spec -2X 0.330 mm diameter) or nylon (VARIVAS Super tippet Master spec 9X 0.074 mm diameter) were used as removable partitions after rinsing with ethanol. Note that the diameter values were provided by the supplier according to measurements by caliper, while by microscopy, the diameters were measured to be 94.3 ± 1.4 and 82.7 ± 1.7 μm instead of 0.086 and 0.074 mm, respectively. For the simplest device, involving one transient partition in an 80 μm-high chamber, the chamber was composed of a 2 mm-wide and 9 mm-long rectangular area that splits at both ends into a thin 70 μm-wide and 8 mm long middle straight channel (guiding duct) surrounded by two 900 μm-wide and 2.5 mm-long channels connected to reservoirs (see Fig. 1a, top). The PDMS block was pierced by a microfilament at both ends of the guiding ducts using a sewing needle, and the microfilament was inserted into the chamber using the ducts as guiding structures (Fig. 1a bottom). The microfilament acted as a partition dividing the chamber into two compartments in a closed configuration (Fig. 1b left). It could be easily removed by pulling one of its extremities with bent tweezers (SMD 21 SA, Xcelite), leading to the open configuration of the chamber (Fig. 1b, right). Other configurations of devices with up to 4 partitions or with a 300 μm-high chamber are illustrated in ESI† (see Results and discussion section).

Cell preparation

The study was carried out in accordance with European Community guidelines on the care and use of laboratory animals: 86/609/EEC. The research purpose and the protocol are described in the Ethical Annex of ERCadg project CellO, which was approved and is regularly reviewed by the ERCEA. Institut Curie animal facility has received licence #C75-05-18, 24/04/2012, reporting to Comité d'Ethique en matière d'expérimentation animale Paris Centre et Sud (National registration number: #59).

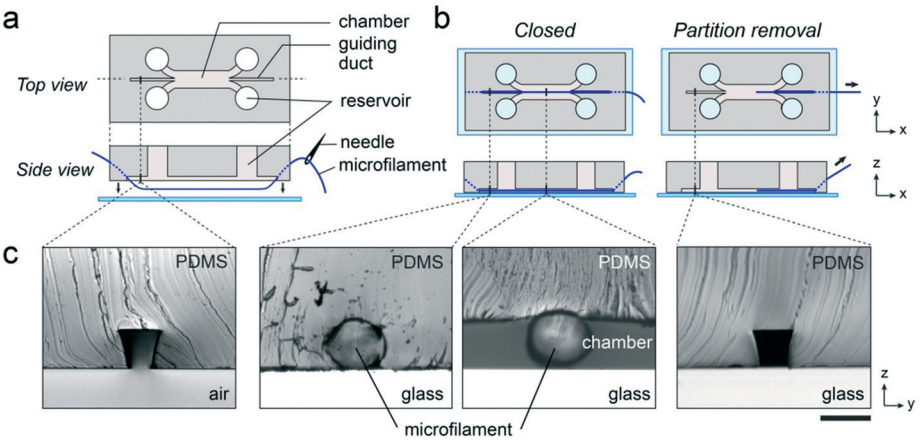

Fig. 1 (a) Scheme of the microfluidic device equipped with a microfilament as a transient partition. (b) The chamber is divided into two compartments by the microfilament (left). The microfilament can be easily removed at any desired moment to transform the chamber into the open configuration. (c) Bright field microscopy images of the cross sections of the microfluidic device at various stages of fabrication and locations (see the dashed black lines toward (a) and (b) schemes). Scale bar, 100 μm.

Madin-Darby canine kidney (MDCK) cells. MDCK cells of wild type (WT, CCL-34 line from ATCC) and those expressing GFP-Lifeact (LA) (stable transfection with Lifeact-TagGFP2 plasmid from Ibidi) were cultured with Dulbecco's modified Eagle medium (DMEM) GlutaMax high glucose containing 10% fetal bovine serum (FBS) (v/v) in 25 cm^2 flasks (TPP) at 37 °C with 5% CO_2 in a humidified CO_2 incubator. For the latter cell type, 0.4 mg mL^{-1} geneticin (Thermo Fisher Scientific) was added to the culture medium. At around 90% confluency, cells were detached using TrypLE Express (Themo Fisher Scientific), rinsed with the culture medium, and re-suspended in 500 μL of the medium with or without geneticin prior to seeding in a chip. The cell density at this stage was measured to be 2×10^7 cells mL^{-1}.

Cortical neurons. Cortices from E17 embryos of B6J mouse expressing tdTomato were dissected on ice under a microscope in L-15 medium without phenol red (Life technologies), supplemented with 0.6% glucose (w/v) and 0.1 mg mL^{-1} gentamycin. After rinsing with the dissection medium, the cortices were digested in papain solution (10 U mL^{-1} papain, 100 U mL^{-1} DNAseI, 0.2 mg mL^{-1} L-cystein, 1.5 mM NaOH, 0.1 mM $CaCl_2$, and 0.5 mM ethylenediaminetetraacetic acid (EDTA) in the dissection medium) at 37 °C for 20 min. The digestion was stopped by aspirating supernatant and rinsing with minimum essential medium (MEM) without glutamine, supplemented with 0.6% glucose (w/v), 1 mM sodium pyruvate, 1% GlutaMAX, and 10% FBS (v/v) (ThermoFisher Scientific except glucose). Cells were mechanically dissociated by pipetting in the rinsing medium containing 100 U mL^{-1} DNAseI, collected by centrifugation at 100 × *g* for 6 min, and suspended in complete culture medium: DMEM GlutaMAX high glucose, supplemented with 10% FBS, 2% B27, 1% N2 (v/v), and 100 U mL^{-1} penicillin–streptomycin (all from ThermoFisher Scientific), at 1.25×10^8 cells per mL.

Glial cells. A 10 cm-diameter polystyrene culture dish (TPP) was incubated with 15 μg mL^{-1} poly-L-ornithine in phosphate buffered saline (PBS) overnight at room temperature and rinsed with PBS prior to use. One hemisphere of an E19 embryo of B6J mouse expressing GFP-Lifeact was dissociated as described above, seeded on the dish and cultured for 2 weeks in DMEM supplemented with 1% GlutaMAX (v/v), 1 mM sodium pyruvate, 0.1 mg mL^{-1} gentamicin, and 10% FBS (v/v) at 37 °C with 5% CO_2 in the incubator. Cells were incubated with 2 mL of 0.05% trypsin–EDTA for 6 min for detachment, rinsed with the complete medium, and re-suspended in the complete medium at the density of 3×10^7 cells mL^{-1} prior to use. All reagents here were obtained from ThermoFisher Scientific.

Sealing test and diffusion assay

A PDMS-coated glass slide was prepared by spreading a degassed PDMS mixture on a glass slide with a spin-coater (SPIN150, SPS-Europe) at 3000 rpm for 30 s, followed by reticulation at 66 °C for at least 4 h. An 80 μm-high chamber equipped with a fluorocarbon microfilament (0.086 mm diameter) was bonded by plasma treatment (Pico PCCE, Diener) to either a glass slide or a PDMS-coated glass slide as the bottom substrate. Immediately after chip assembly, 20 μL of 10 μM fluorescein in PBS was introduced into the two reservoirs connected to one transient compartment, and 20 μL of PBS into the two reservoirs connected to the other compartment. The solutions spontaneously filled the channels and the chamber due to their hydrophilic surface property. To investigate sealing efficiency, both types of chips were sealed in a Petri dish containing a few mL drop of PBS to avoid evaporation. The leakage of fluorescein into the other compartment was evaluated by fluorescence microscopy after 24 h of incubation at room temperature while maintaining the microfilament in place. To investigate the diffusion of fluorescein triggered by microfilament removal, the filament was removed from a glass-bottom device under fluorescence microscopy observation 10 min after filling the reservoirs. A numerical simulation of fluorescein diffusion was performed using COMSOL Multiphysics software.

Surface co-coating

An 80 μm-high chamber equipped with a fluorocarbon microfilament (0.086 mm diameter) was bonded on a glass cover slip using plasma treatment. In a first experiment, 20 μL of 0.01 mg mL^{-1} fluorescein isothiocyanate-labeled poly(L-lysine) (PLL-FITC) in PBS was introduced into one compartment, and 20 μL of 0.01 mg mL^{-1} PLL grafted with poly(ethylene glycol) and tetramethylrhodamine isothiocyanate (PLL-*g*-PEG/TRIC, SuSoS AG) in PBS was introduced into the other compartment, immediately after chip assembly by plasma bonding. The chip was sealed in a Petri dish with a few mL drop of PBS, and incubated for 1 h at room temperature. Solutions in the reservoirs were then removed by micropipette and the chamber was rinsed with PBS. After removing the microfilament, all the reservoirs were emptied by micropipette and filled with 10 μL each of the PLL-*g*-PEG/TRIC solution. After 1 h incubation at room temperature, the chamber was rinsed with PBS and the surface of the bottom substrate was observed by confocal microscopy. In a second experiment with MDCK LA cells, PLL-FITC was replaced with non-fluorescent poly(D-lysine) (PDL). After rinsing the chamber with culture medium for MDCK cells, 1 μL each of MDCK LA cell suspension was introduced from two upstream reservoirs to the chamber. At this stage, cells were homogeneously distributed in the chamber. After 10 min incubation in the CO_2 incubator, all the reservoirs were filled with 40 μL each of culture medium with geneticin and cells were cultured in the incubator.

Two dimensional cell co-culture in the device on a culture dish

An 80 μm-high chamber equipped with a nylon microfilament was placed on a polystyrene culture dish (TPP) and pressed down to be in good contact with the dish bottom (see ESI† Fig. S3 for detailed illustration). 40 μL of culture

medium was then introduced into the two upstream reservoirs. Using a 1 mL disposable syringe (Terumo), the medium was sucked from the downstream reservoirs. Once the chamber was filled, the medium remaining in all the reservoirs was removed by micropipette. 3 μL of MDCK WT and LA cell suspensions, respectively, were introduced in the two upstream reservoirs. The culture dish was enclosed in a larger Petri dish with a few mL drop of water and kept in a CO_2 incubator for 1 h to make cells adhere on the culture dish surface. The microfilament was then removed by using two sets of tweezers, one for pressing down the device and the other to remove the filament. All reservoirs were filled with 40 μL of culture medium for MDCK cells without geneticin, and cells were cultured for 2 days in the incubator.

Three dimensional co-culture of neurons and glial cells in hydrogel compartments

An 80 μm-high microfluidic chamber equipped with 4 fluorocarbon microfilaments (0.086 mm diameter), *i.e.* with 5 compartments, was bonded on a glass cover slip using plasma treatment. Collagen I from rat tail, 10× PBS, sodium hydroxide, ECM gel, and complete medium were mixed and kept on ice. Cell suspension of one-fifth of the final volume was added and mixed immediately before the introduction to the device. The final concentration of collagen I and sodium hydroxide were 2 mg mL^{-1} and 8 mM, respectively. The final volume fraction of ECM gel was 25%. To form a cell-laden hydrogel slab in a transient compartment, 10 μL of hydrogel precursor containing cells was placed next to an inlet of the compartment, at the bottom of a reservoir. To fill the compartment, the solution was sucked from the other reservoir connected to the same compartment using a 1 mL disposable syringe. Once the compartment was filled, the device was enclosed in a plastic box containing 1 mg mL^{-1} EDTA to avoid evaporation and incubated at 37 °C for 30 min in the CO_2 incubator for gelation. To form continuous hydrogel slabs, the microfilament between two slabs was removed between the gelation steps of those slabs (see Results and discussion section). The reservoirs and the remaining compartments were filled with the complete culture medium and cells were cultured in the CO_2 incubator.

Imaging

Sample observations were made by fluorescence microscopy (Eclipse Ti, Nikon) equipped with a CCD camera (CoolSNAP HQ2, Photometrics) or by confocal microscopes (LSM 510 Meta, Zeiss; TCS SP8, Leica). Images were analyzed using ImageJ software.

Results and discussion

1. Principle of microfilament-based compartmentalization

A demonstration of the principle of our microfilament-based technology to partition micro-chambers is shown in Fig. 1a. The microfluidic device is equipped with a single transient partition, *i.e.* a cylindrical microfilament, inserted in a main chamber. As described in the previous section, the microfilament was embedded in the device using a sewing needle so that the paths of the filament outside the chamber and guiding ducts were sealed spontaneously without leaving open holes after filament removal. After chip assembly, the filament divided the chamber into two transient compartments, being pinched between the chamber ceiling and the bottom substrate. The microfilament can slide freely along the guiding ducts and the chamber axis; to open the partition, the filament is simply pulled out from the device by one of its ends (Fig. 1b). To achieve an efficient partition, the diameter of the microfilament (94.3 ± 1.4 μm) was chosen slightly larger than the height of the duct and the chamber (82.8 ± 3.0 μm), and the width of the duct (70 μm).

In order to characterize the *in situ* geometry of the sealing, cross sections of the device at different stages were imaged. The cross section of an empty guiding duct before chip assembly was first obtained (Fig. 1c left). Next, the cross sections of the guiding duct and the microfluidic chamber after chip assembly by plasma bonding were observed (Fig. 1c middle). As shown in these images, the microfilament completely filled the guiding duct and was also in direct contact with the ceiling of the chamber, which was as expected slightly deformed by the microfilament. The cross section of the guiding duct after microfilament removal, *i.e.* in the open configuration, was then observed, proving that the duct recovered its original shape (Fig. 1c right). It was also evidenced that the microfilament did not disturb the bonding between PDMS and the glass substrate.

So far, up to 4 partitions could be inserted in a microfluidic chamber of the same height without difficulty. Fig. S1 in ESI† shows the designs of microfluidic chambers with 1 to 4 partitions with their positions indicated. The detailed procedure to insert 4 microfilaments in a chamber, which results in creating 5 transient compartments, is illustrated in Fig. S2 in ESI.†

2. Long-term sealing efficiency

A long-term sealing efficiency of the partition was investigated by observing the leakage of fluorescein from one transient compartment to the other after 24 h. A small leakage was qualitatively observed in a standard glass-bottom device (Fig. 2a left). The profile of the fluorescence intensity integrated along the chamber is shown in Fig. 2b (i), the intensity value being normalized to a total area sum of 100. The fluorescence intensity in the right compartment due to the leakage was 16.4 ± 9.4% of the total intensity of both compartments (6 samples). This limited long-term leakage could potentially be the consequence of incomplete sealing between the microfilament and the glass substrate, both being hard materials. To test this hypothesis and to improve the device efficiency, the same experiment as above was conducted replacing the bottom substrate with a PDMS-coated glass slide (Fig. 2a right). The thickness of the PDMS layer was

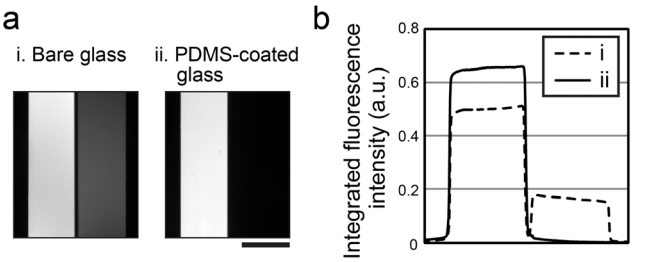

Fig. 2 Long-term sealing efficiency. (a) Fluorescence microscopy images of a chamber divided by a microfilament with a glass slide (i) or with a PDMS-coated glass slide (ii) as the bottom substrate, 24 h after filling the left compartment with fluorescein solution. Leakage of fluorescein is observed only with the glass-bottom chip. (b) Profiles of integrated fluorescence intensities of the images shown in (a), normalized to area sum equal to 100. Scale bar, 1 mm.

measured to be 30.2 ± 0.4 μm. As plotted in Fig. 2b, the elastomeric property of the bottom substrate was sufficient to achieve full sealing, as we did not observe any leakage of fluorescein after 24 h. This result was obtained reproducibly, proving that complete long-term sealing can be achieved by working with a thin PDMS layer on the bottom substrate if desired. It is worth mentioning that the presence of a PDMS layer does not limit the use of this device for cell culture, as demonstrated previously.[13] In the following applications, however, we use non-coated substrates only, since the sealing efficiency of the microfilament partition is high enough (less than 1% of leakage) for 1 h, a typical incubation time for our experiments.

3. Triggerable chemical diffusion

Besides static compartmentalization, the removable microfilament strategy can also be dynamically used in biochemical and cellular assays, by opening the partition at the desired time, in order to diffuse molecules from one compartment to the other. To investigate this aspect, we confined a fluorescein aqueous solution in one compartment and observed its diffusion during and after filament removal in a glass-bottom 2-compartment device. As shown in Movie S1 in ESI,† the filament removal only disturbed the interface between the two solutions on a scale of the order of the microfilament diameter. A series of fluorescence microscopy images illustrate fluorescein diffusion after the chamber opening (Fig. 3a). To evaluate the influence of microfilament removal on fluorescein diffusion, these experimental observations were compared with a numerical simulation. The fluorescence intensity profile obtained immediately after filament removal was used as the initial fluorescein concentration distribution in the channel section, and the diffusion of fluorescein was computed for 120 s with its diffusion coefficient, 4.25×10^{-10} m^2 s^{-1}.[42] The theoretical data were compared with the experimental fluorescence intensity profiles obtained at various time points along a transversal line of the chamber. As shown in Fig. 3b, we obtained a good agreement between experimental and simulation data. A small discrepancy was observed between the experimental curve for t = 120 s (red line) and the theoretical values (open diamonds), which might be due to the small transversal flow filling the space of the microfilament after its removal. However, the characteristic features of diffusion are finally well conserved.

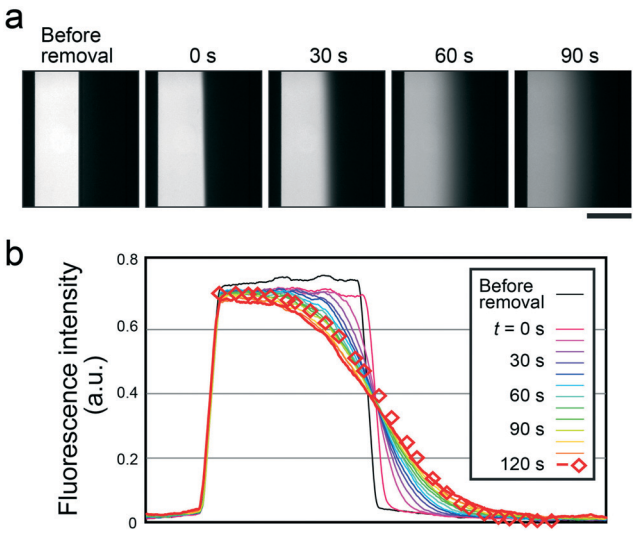

Fig. 3 Triggerable chemical diffusion. (a) Fluorescence microscopy images of a glass-bottom chamber containing fluorescein, which was initially introduced in the left transient compartment, before and after removal of a microfilament. (b) Fluorescence intensity profiles normalized to area sums equal to 100 at various time points, t, along a transversal line in the chamber (solid lines), and the result of a numerical simulation corresponding to t = 120 s starting from the experimental data at t = 0 s (open diamonds). The simulation was performed in an 80 μm-high, 2 mm-wide, and 3 mm-long cuboid mimicking the chamber. Scale bar, 1 mm.

This experiment shows the potential of our method to perform chemical stimulation with negligible flow perturbation, in a configuration allowing continuous recording. This can find various applications, in particular for the chemical or biochemical stimulation of cells sensitive to shear, or even more fragile objects, such as giant unilamellar vesicles.[43] As described below, the device can be composed of more than two compartments, thus enabling multi-step stimulations simultaneously or sequentially.

4. Surface co-coating

We further validated that the strategy was efficient enough to compartmentalize aqueous solutions of various compositions performing surface co-coating by means of transient partitioning. As an example, we incubated one compartment on a glass substrate with cell adhesive PLL-FITC and the other with cell repellent PLL-*g*-PEG/TRIC, respectively, using a 2-compartment device (Fig. 4a). After removal of the microfilament, a gap of a few tens of μm was left between the two coated areas, due to the coverage of the glass slide by the filament during the coating process. In order to achieve a sharp interface, this gap was filled after filament removal with the latter molecule by a second coating step performed in the

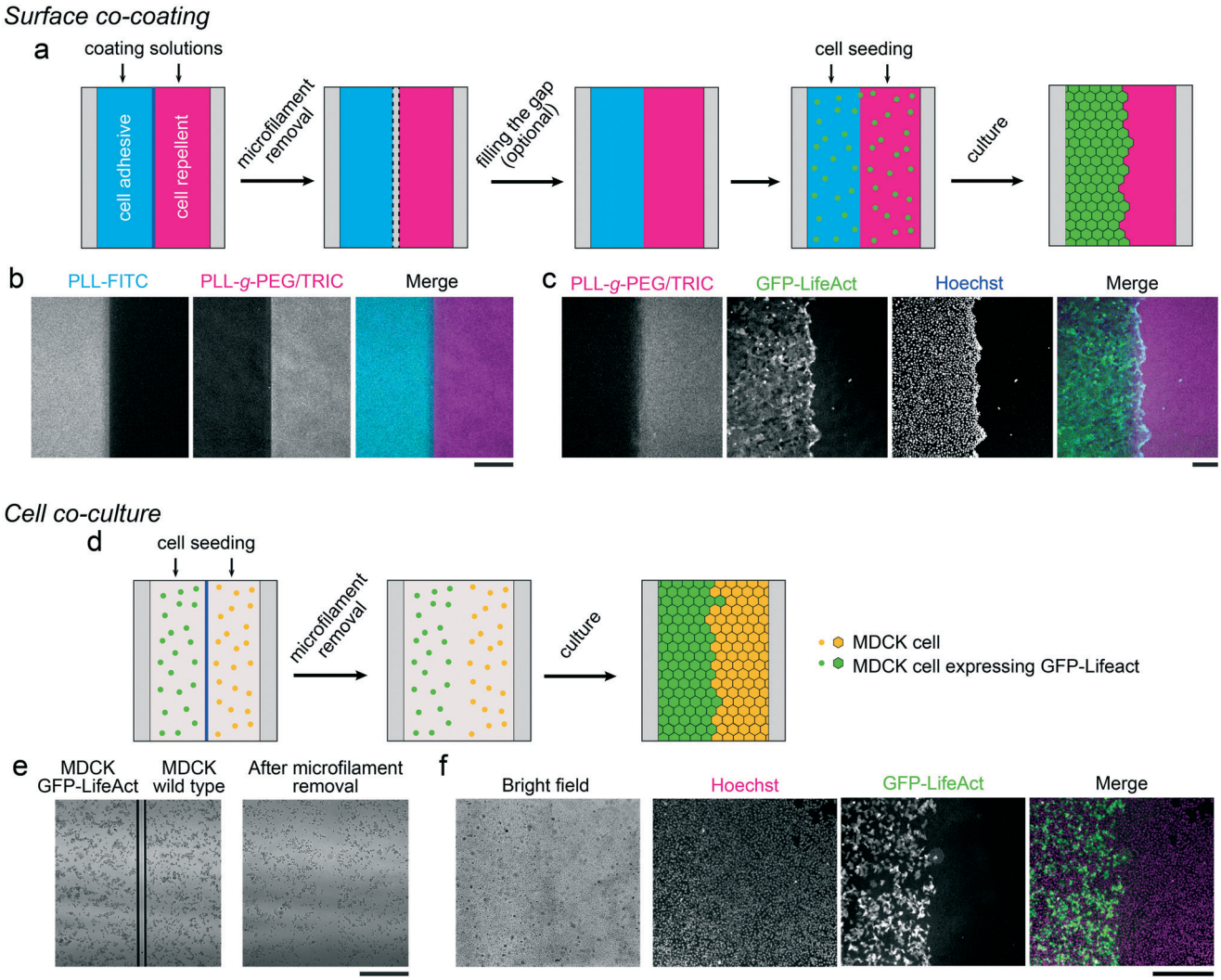

Fig. 4 (a–c) Surface co-coating using the device on a glass slide. (a) Scheme of the experiment. (b) Confocal microscopy images of a glass substrate at the bottom of the device coated with PLL-FITC (cyan) and PLL-*g*-PEG/TRIC (magenta). (c) Confocal microscopy images of MDCK cells expressing GFP-LifeAct (green) and their nuclei stained with Hoechst (blue), after 3 days of culture in the device coated with non-fluorescent PDL and PLL-*g*-PEG/TRIC (magenta). Geneticin antibiotic selection was maintained during the experiment. (d–f) 2D cell co-culture in the device directly placed on a culture dish. (d) Scheme of the experiment. A plastic-bottom cell culture dish was used as the bottom substrate of the device. (e) Bright field microscopy images after seeding two different cell populations in transient compartments separated by a microfilament (left) and after the removal of the filament (right). (f) From the left, a bright field microscopy image of cells, fluorescence microscopy images of nuclei (Hoechst), GFP-LifeAct, and their merge, taken after 2 days of culture. Cells were cultured in a medium without geneticin selection due to the presence of WT cells after seeding. Scale bars, 200 μm (b and c) and 500 μm (e and f).

whole chamber, as described above. Confocal images (Fig. 4b) evidence the efficiency of this approach, displaying a sharp interface between the two areas and a homogeneous coating within each area. To further demonstrate the functionality of the co-coated substrate, MDCK LA cells were introduced into a device prepared with non-fluorescent PDL instead of PLL-FITC. As expected, cells grew and covered the adhesive surface (PDL coated area), whereas they did not adhere to the repellent surface, and flowed away during culture medium supply (Fig. 4c).

This simple co-coating strategy is applicable for other biopolymers or proteins, as well as different substrates including culture dishes, providing a platform that enables a direct comparison of cell responses on differently coated substrates in a single chip. In contrast to previous technologies, our strategy does not require fluidic control and provides homogeneously coated areas without ambiguous interface with a gradient.[26,27]

5. Microfluidic two dimensional cell co-culture on a culture dish

The same principle can be easily applied to compartmentalize cells in a chamber. It allows one to seed and grow multiple cell populations in defined positions in a single chamber, for instance to study intercellular communication *via*

secretion, to perform invasion assays, or to perform wound healing assays by removing the microfilament after reaching cell confluency.[28–31,33] To demonstrate this potential as well as the compatibility of our approach with conventional biological supports, we used a standard polystyrene culture dish as a bottom substrate, the cell positioning being imposed by the microfluidic chamber and partition. The PDMS part of the device, with its microfilament in position, was simply pressed down on the dish bottom without any plasma treatment. Therefore, the PDMS device and the culture dish were bonded simply by van der Waals forces. Importantly, a nylon microfilament with a smaller diameter (82.7 ± 1.7 μm) was used here to keep a good contact between the PDMS and the culture dish, which were less strongly bonded as compared to plasma bonding. As illustrated in Fig. S3 in ESI,† the hydrophobic property of the bottom substrate interrupted neither medium introduction nor cell seeding. No medium leakage was observed. In this experiment, the filament was removed 1 h after cell seeding, when the cells adhered to the dish but had not started proliferating (Fig. 4d and e). At 2 days *in vitro* (DIV), cells proliferated and covered the whole substrate in the chamber, while preserving the initial partitioning of the populations (Fig. 4f).

As demonstrated here, one can easily integrate the device into standard cell culture processes, owing to the versatility of our approach regarding the material of the bottom substrate. This simple strategy provides new miniaturized platforms for 2D cell co-cultures embedded in microfluidic devices with controlled microenvironments, with the possibility to remove the partition at any moment, to seed cells at different time points, and/or to vary the density of cells as needed for instance for cell competition assays. The simplicity of the approach, and in particular the possibility to operate it with a device reversibly bonded to a substrate, also opens new opportunities for biopatterning protocols involving complex and time-extended processes.

6. Three dimensional co-culture of neurons and glial cells in hydrogel compartments

Finally, to meet the growing demand to create biomimetic cellular microenvironments, as stated above, the potential of our approach to obtain parallel cell-laden hydrogels for 3D cell co-culture has been investigated. In particular, we performed in a 5-compartment configuration a 3D co-culture of mouse primary neurons and glial cells, embedded in ECM-mimicking hydrogels at well-defined positions. A 2.2 mm-wide chamber was split into five 500 μm-wide channels connected to reservoirs at both ends (Fig. 5a left). In this case, instead of narrow guiding ducts, the channel walls served as guiding structures for the microfilaments. As illustrated in Fig. 5a, firstly, the 2nd and 4th compartments were filled with a hydrogel precursor containing neurons prior to gelation at 37 °C for 30 min in the CO_2 incubator. Next, the 3rd compartment was filled with a hydrogel precursor containing glial cells. Prior to gelation of the newly-introduced hydrogel precursor, the microfilaments separating hydrogels from the middle phase were removed so that the precursor was in contact with the gel phases. Once the middle phase was gelled, the 1st and 5th compartments were filled with complete culture medium, followed by removal of the remaining filaments. All reservoirs were filled with the complete medium during cell culture.

As shown in Fig. 5b, at 6 DIV, the two populations of neurons in the 2nd and 4th compartments have formed a network of neurites that reached each other across the central glial compartment (enlarged image in ESI† Fig. S4). Moreover, glial cells in the middle compartment formed clusters along the neurites, and partially migrated into the neuron compartments. To further observe the 3D distribution of these cells, we performed confocal microscopy observations. As shown in Fig. 5c and d, both neurons and glial cells were distributed along the height as well as in lateral directions, interacting with each other. These results clearly demonstrate that continuous hydrogel compartments were successfully formed, enabling the cells from different compartments to mutually interact and to form a 3D network structure in the device. A perhaps more evident representation of the height distribution of the neurons is shown in Fig. 5e, where it can be observed that they partially reach the ceiling of the chamber. Compared to neurons, glial cells tended to be closer to the bottom surface in this condition, due to their higher density as seen in Fig. 5d bottom left. Nonetheless, although there were glial cells adhering partly or completely to the bottom substrate, part of the population was entirely embedded in ECM. Interestingly, some of those cells formed protrusions in all directions, a characteristic shape of astroglia (Fig. 5f). Moreover, we observed a clear co-localization of a neurite (or a bundle of neurites) and glial cells directly in the hydrogel matrix (Fig. 5g). Fluorescence of the glial cells corresponding to GFP-Lifeact confirms the presence of significant amounts of actin in the glial cells along the neurite. It is worth mentioning that actin indeed plays an important role in the myelination of axons by glial cells.[44] Such a phenomenon is difficult to reproduce in a 2D culture, where all the cells are tightly adhering on a substrate. In contrast, our system enables to form a complex 3D network of these cell types in a spatially controlled manner.

This method presents the advantage of not being sensitive to the viscosity of the hydrogel precursors, gelation temperature or gelation time, nor to the wettability of the chamber surface, making it universally applicable to a wide variety of hydrogels. To highlight this advantage, we achieved hydrogel compartments from rat tail collagen I at different densities in a 3-compartment device. As shown in Fig. S5 in ESI,† collagen networks with different properties were formed uniformly in each compartment, while being in direct contact with each other (see Text S1 in ESI† for the method). Increasing the chamber height is also an interesting option, allowing not only an increase in the number of cells embedded in the hydrogel, but also the use of the device for embedding larger

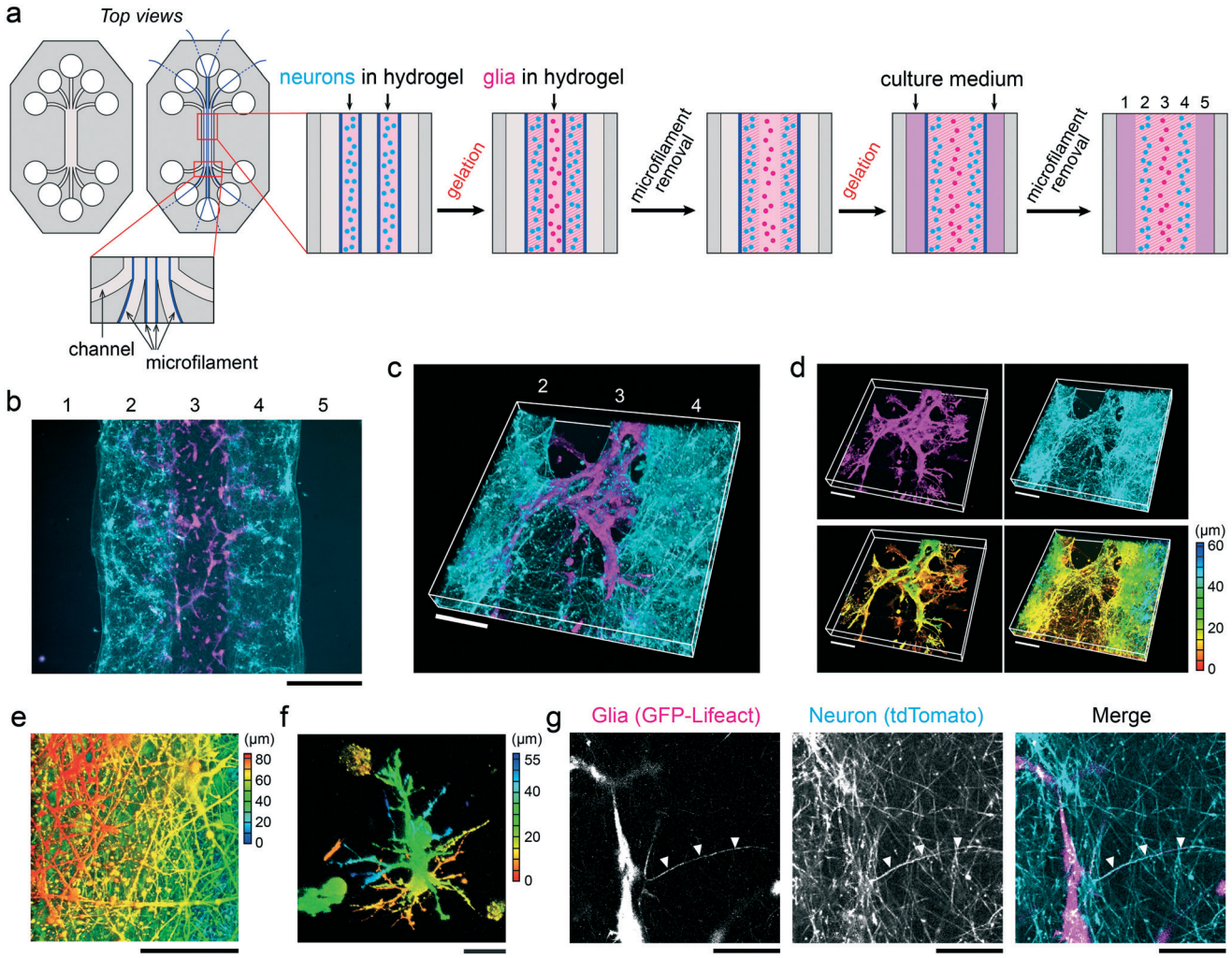

Fig. 5 3D co-culture of neuron and glial cells. (a) Scheme of the device with 5 transient compartments (left), and the process to construct continuous hydrogel compartments containing neurons expressing tdTomato and glial cells expressing GFP-Lifeact, respectively (right). (b) Fluorescence microscopy image of the chamber with neurons (tdTomato, cyan) and glial cells (GFP-Lifeact, magenta) at 6 days *in vitro* (DIV). The numbers on the image correspond to those in (a). (c) 3D reconstruction of confocal images of neurons (cyan) and glial cells (magenta) at the middle of the chamber at 6 DIV. (d) Separate 3D reconstructions of glial cells (top left) and neurons (top right) images identical to (c), and those with depth-coding colors (bottom). (e) 3D reconstruction of confocal images of neurons at a higher magnification with depth-coding colors. (f) 3D reconstruction of confocal images of glial cells at a higher magnification with depth-coding colors. (g) Confocal microscopy images of glial cells (left), neurons (middle), and their merge (right) at the height of 18 μm from the bottom of the device at 6 DIV. Arrowheads indicate the co-localization of glia and neuronal protrusions. Scale bars, 500 μm (b), 100 μm (c–e and g), and 20 μm (f).

cellular structures, such as spheroids, tumoroids, and organoids. In this context, we fabricated a 300 μm-high bovine collagen I slab in a newly designed chamber (ESI† Fig. S6). The slab sandwiched by aqueous phases was stable after microfilament removal, and presented a sharp interface.

By taking advantage of these features, the microfilament approach can be applied to a wide range of studies, such as cellular response to hydrogels with different rigidities or compositions in a single chamber, communications between separate cell populations *via* secretion or mechanical forces, and 3D reconstitution of biomimetic cellular architectures with multiple cell populations in the context of organ-on-a-chip devices. The unique versatility of our approach provides an easy solution for such studies, previously difficult with other techniques, limited by hydrogel or surface properties and by complex handling.[38–41,45]

Conclusions

In this study, we described a strategy to transiently create different fluidically isolated domains in microfluidic chambers, and remove these partitions at arbitrary times. Its successful applications ranging from molecular compartmentalization to 3D cell co-culture were demonstrated. This strategy presents various advantages with regards to previous ones involving pressure-controlled valves, laminar flow or multiphasic fluids. First, the microfabrication is simple: it requires neither multilayer lithography, nor alignment. Second,

it allows the creation of sharp interfaces on centimeter lengths, and high aspect ratio boundaries. The method is also insensitive to the composition or viscosity of the fluids to compartmentalize, making it robust and easy to implement. By adding a thin layer of PDMS on the bottom substrate, a complete sealing of the compartments by the partition can be achieved for days. The technology is also versatile regarding the substrate: we could use glass slides and plastic-/glass-bottom cell culture dishes as a substrate, with and without plasma bonding, thus providing a high flexibility regarding assay format and surface treatments. All the steps of chip preparation, sample introduction, and partition removal were easy to perform, making the technology robust and applicable in a wide range of environments, including biology laboratories without sophisticated microfluidic tools. Since surface treatment or hydrogel formation is performed in flow-free conditions, reagents consumption is very limited. Finally, as compared *e.g.* to pressure-based valves, the device can be handled manually, and does not require connection to a pressure source. It can thus be handled and stored freely before or after partition removal. This is a key advantage in particular for cell biology experiments, in which a multiplicity of devices must be kept in an incubator for long periods of time, and intermittently transported *e.g.* to a microscope equipment for inspection. In addition, if desired, the number of compartments can be further increased by working on an incremental design of ESI† Fig. S6, *i.e.* by placing straight compartments and guiding ducts alternately.

Acknowledgements

We thank Floriane Cohen, Guillaume Laffite, Fanny Cayrac, and Anne-Christine Brunet for their help with our experiments. We thank Caterina Tomba for providing the protocol for glial cell culture. We thank Danijela Vignjevic for providing the tdTomato mice, Pablo Vargas and Ana-Maria Lennon for providing the GFP-LifeAct mice, Isabelle Grandjean and Manon Chartier from the Animal Facility of Institut Curie for their crucial support for mice. This work was performed in part in the technology platform of Institut Pierre-Gilles de Gennes, in UMR 168 microfabrication cleanroom, and in Bio-Imaging Cell and Tissue Core Facility (PICT-IBiSA) of Institut Curie. This work was supported by ANR "Investissements d'Avenir" for Labex and Equipex IPGG (ANR-10-LABX-31 and ANR-10-IDEX-0001-02-PSL), and grants from the European Commission: MicroDEG, ERA-NET Neuron JTC2012 "Novel Methods", http://www.neuron-eranet.eu/en/317.php, and ERC Advanced Grant CellO (FP7-IDEAS-ERC-321107). BV acknowledges support from DGA.

Notes and references

1 M. A. Unger, H. P. Chou, T. Thorsen, A. Scherer and S. R. Quake, *Science*, 2000, **288**, 113–116.
2 K. Eyer, S. Stratz, P. Kuhn, S. K. Kuster and P. S. Dittrich, *Anal. Chem.*, 2013, **85**, 3280–3287.
3 Q. Zhou, D. Patel, T. Kwa, A. Haque, Z. Matharu, G. Stybayeva, Y. Gao, A. M. Diehl and A. Revzin, *Lab Chip*, 2015, **15**, 4467–4478.
4 Y. Gao, D. Majumdar, B. Jovanovic, C. Shaifer, P. C. Lin, A. Zijlstra, D. J. Webb and D. Li, *Biomed. Microdevices*, 2011, **13**, 539–548.
5 W. Du, L. Li, K. P. Nichols and R. F. Ismagilov, *Lab Chip*, 2009, **9**, 2286–2292.
6 A. Yamada, F. Barbaud, L. Cinque, L. Wang, Q. A. Zeng, Y. Chen and D. Baigl, *Small*, 2010, **6**, 2169–2175.
7 K. A. Heyries, C. Tropini, M. Vaninsberghe, C. Doolin, O. I. Petriv, A. Singhal, K. Leung, C. B. Hughesman and C. L. Hansen, *Nat. Methods*, 2011, **8**, 649–651.
8 M. K. Verma, A. Majumder and A. Ghatak, *Langmuir*, 2006, **22**, 10291–10295.
9 N. Mori, Y. Morimoto and S. Takeuchi, *Proc. μTAS*, 2015.
10 X. Li, J. Tian and W. Shen, *ACS Appl. Mater. Interfaces*, 2010, **2**, 1–6.
11 M. Reches, K. A. Mirica, R. Dasgupta, M. D. Dickey, M. J. Butte and G. M. Whitesides, *ACS Appl. Mater. Interfaces*, 2010, **2**, 1722–1728.
12 R. Safavieh, G. Z. Zhou and D. Juncker, *Lab Chip*, 2011, **11**, 2618–2624.
13 A. Yamada, M. Vignes, C. Bureau, A. Mamane, B. Venzac, S. Descroix, J. L. Viovy, C. Villard, J. M. Peyrin and L. Malaquin, *Lab Chip*, 2016, **16**, 2059–2068.
14 K. W. Oh and C. H. Ahn, *J. Micromech. Microeng.*, 2006, **16**, R13–R39.
15 J. C. Galas, D. Bartolo and V. Studer, *New J. Phys.*, 2009, **11**, 075027.
16 P. B. Allen and D. T. Chiu, *Biochim. Biophys. Acta*, 2008, **1782**, 326–334.
17 N. Bhattacharjee, N. Li, T. M. Keenan and A. Folch, *Integr. Biol.*, 2010, **2**, 669–679.
18 M. Morel, V. Shynkar, J. C. Galas, I. Dupin, C. Bouzigues, V. Studer and M. Dahan, *Biophys. J.*, 2012, **103**, 1648–1656.
19 C. J. Wang, X. Li, B. Lin, S. Shim, G.-L. Ming and A. Levchenko, *Lab Chip*, 2008, **8**, 227–237.
20 H. Shin, S. Jo and A. G. Mikos, *Biomaterials*, 2003, **24**, 4353–4364.
21 Y. Xia and G. M. Whitesides, *Angew. Chem., Int. Ed.*, 1998, **37**, 550–575.
22 B. Lom, K. E. Healy and P. E. Hockberger, *J. Neurosci. Methods*, 1993, **50**, 385–397.
23 H. Sorribas, C. Padeste and L. Tiefenauer, *Biomaterials*, 2002, **23**, 893–900.
24 A. Azioune, M. Storch, M. Bornens, M. Thery and M. Piel, *Lab Chip*, 2009, **9**, 1640–1642.
25 P. O. Strale, A. Azioune, G. Bugnicourt, Y. Lecomte, M. Chahid and V. Studer, *Adv. Mater.*, 2016, **28**, 2024–2029.
26 S. K. Dertinger, X. Jiang, Z. Li, V. N. Murthy and G. M. Whitesides, *Proc. Natl. Acad. Sci. U. S. A.*, 2002, **99**, 12542–12547.
27 L. J. Millet, M. E. Stewart, R. G. Nuzzo and M. U. Gillette, *Lab Chip*, 2010, **10**, 1525–1535.
28 J. Behrens, P. Kameritsch, S. Wallner, U. Pohl and K. Pogoda, *Eur. J. Cell Biol.*, 2010, **89**, 828–838.

29 P. Chieng-Yane, A. Bocquet, R. Létienne, T. Bourbon, S. Sablayrolles, M. Perez, S. N. Hatem, A.-M. Lompré, B. Le Grand and M. David-Dufilho, *J. Pharmacol. Exp. Ther.*, 2010, **336**, 643–651.
30 A. Msaki, A. M. Sanchez, L. F. Koh, B. Barre, S. Rocha, N. D. Perkins and R. F. Johnson, *Mol. Biol. Cell*, 2011, **22**, 3032–3040.
31 Y.-T. Shih, M.-C. Wang, H.-H. Peng, T.-F. Chen, L. Chen, J.-Y. Chang and J.-J. Chiu, *Cell. Signalling*, 2012, **24**, 779–793.
32 S. R. K. Vedula, H. Hirata, M. H. Nai, A. Brugues, Y. Toyama, X. Trepat, C. T. Lim and B. Ladoux, *Nat. Mater.*, 2014, **13**, 87–96.
33 M. Poujade, E. Grasland-Mongrain, A. Hertzog, J. Jouanneau, P. Chavrier, B. Ladoux, A. Buguin and P. Silberzan, *Proc. Natl. Acad. Sci. U. S. A.*, 2007, **104**, 15988–15993.
34 J. B. Wu, M. Y. Zhang, L. Q. Chen, V. Yu, J. T. Y. Wong, X. X. Zhang, J. H. Qin and W. J. Wen, *RSC Adv.*, 2011, **1**, 746–750.
35 F. Pampaloni, E. G. Reynaud and E. H. Stelzer, *Nat. Rev. Mol. Cell Biol.*, 2007, **8**, 839–845.
36 J. Patterson, M. M. Martino and J. A. Hubbell, *Mater. Today*, 2010, **13**, 14–22.
37 S. Ghosh, G. C. Spagnoli, I. Martin, S. Ploegert, P. Demougin, M. Heberer and A. Reschner, *J. Cell. Physiol.*, 2005, **204**, 522–531.
38 A. P. Wong, R. Perez-Castillejos, J. Christopher Love and G. M. Whitesides, *Biomaterials*, 2008, **29**, 1853–1861.
39 A. Kunze, M. Giugliano, A. Valero and P. Renaud, *Biomaterials*, 2011, **32**, 2088–2098.
40 Y. Shin, S. Han, J. S. Jeon, K. Yamamoto, I. K. Zervantonakis, R. Sudo, R. D. Kamm and S. Chung, *Nat. Protoc.*, 2012, **7**, 1247–1259.
41 I. K. Zervantonakis, S. K. Hughes-Alford, J. L. Charest, J. S. Condeelis, F. B. Gertler and R. D. Kamm, *Proc. Natl. Acad. Sci. U. S. A.*, 2012, **109**, 13515–13520.
42 C. T. Culbertson, S. C. Jacobson and J. M. Ramsey, *Talanta*, 2002, **56**, 365–373.
43 A. Yamada, S. Lee, P. Bassereau and C. N. Baroud, *Soft Matter*, 2014, **10**, 5878–5885.
44 J. B. Zuchero, M. M. Fu, S. A. Sloan, A. Ibrahim, A. Olson, A. Zaremba, J. C. Dugas, S. Wienbar, A. V. Caprariello, C. Kantor, D. Leonoudakis, K. Lariosa-Willingham, G. Kronenberg, K. Gertz, S. H. Soderling, R. H. Miller and B. A. Barres, *Dev. Cell*, 2015, **34**, 608.
45 H. Lee and D. W. Cho, *Lab Chip*, 2016, **16**, 2618–2625.